Hydrological data and modeling to combine and validate precipitation datasets relevant to hydrological applications

Alberto Assis Dos Reis, Albrecht Weerts, Maria-Helena Ramos, Fredrik Wetterhall, Wilson dos Santos Fernandes

Journal of Hydrology: Regional Studies 44 (2022) 101200

Contents lists available at ScienceDirect

Journal of Hydrology: Regional Studies

journal homepage: www.elsevier.com/locate/ejrh

Hydrological data and modeling to combine and validate precipitation datasets relevant to hydrological applications

Alberto Assis dos Reis [a,b,*], Albrecht Weerts [c,d], Maria-Helena Ramos [e], Fredrik Wetterhall [f], Wilson dos Santos Fernandes [a]

[a] *Universidade Federal de Minas Gerais, Belo Horizonte, Brazil*
[b] *CEMIG Energy Company of Minas Gerais, Belo Horizonte, Brazil*
[c] *Deltares, Delft, the Netherlands*
[d] *Hydrology and Quantitative Water Management Group, Wageningen University, Wageningen, the Netherlands*
[e] *Université Paris-Saclay, INRAE, UR HYCAR, Antony, France*
[f] *European Centre for Medium-Range Weather Forecasts, Shinfield Park, Reading RG2 9AX, UK*

A R T I C L E I N F O

Keywords:
Precipitation
Hydrological model
Data uncertainty
TRMM-MERGE
CPC-NOAA

A B S T R A C T

Study Region: Forty-one river basins in Brazil and neighboring countries in South America.
Study Focus: In large river basins, on countrywide or continental scales, it is often difficult to have consistent and accurate long time series of spatially distributed precipitation data available. However, these are needed to calibrate hydrological models and to run hydrological simulations continuously in real-time streamflow forecasting. In this study, we assess two real-time precipitation products based on rain gauges and satellite data (TRMM-MERGE and CPC-NOAA) for their use in streamflow forecasting in the hydropower sector in Brazil. To take advantage of each precipitation data source and derive a unique dataset, a methodology is proposed to combine, extend, and validate the datasets. We consider the discharges at the river basin outlets as an independent and robust reference for hydrological applications. Observed discharges are used to quantify precipitation uncertainties and to weight the blending, while discharges obtained from hydrological modeling are used to validate the final precipitation product.
New Hydrological Insights for the Region: The proposed blending method, which uses the uncertainty of the original datasets to define the weighting factors, was efficient in generating a precipitation product that performs better than each dataset separately when used to force a hydrological model. The use of the double-mass curve correlation to extend the time series of the datasets beyond their common period allowed us to produce long time series of precipitation for South American basins and hydrological applications. The study shows that it is possible to rely on river discharge data and hydrological modeling to select and combine different precipitation products in the region and presents a step-by-step methodology to do so.

1. Introduction

Time series of quantitative precipitation estimates is crucial for calibrating and running hydrological models to be used in research

* Corresponding author at: Universidade Federal de Minas Gerais, Belo Horizonte, Brazil.
E-mail addresses: betoreis@cemig.com.br (A.A. Reis), Albrecht.Weerts@deltares.nl (A. Weerts), maria-helena.ramos@inrae.fr (M.-H. Ramos), Fredrik.Wetterhall@ecmwf.int (F. Wetterhall), wilson@ehr.ufmg.br (W.S. Fernandes).

https://doi.org/10.1016/j.ejrh.2022.101200
Received 29 June 2021; Received in revised form 12 July 2022; Accepted 3 September 2022
Available online 9 September 2022

and operational applications such as water resource management, irrigation planning, hydropower operations, and forecasting of floods and droughts. However, in large river basins or on countrywide and continental scales, it is often difficult to have consistent and accurate time series of spatially distributed precipitation data available over a long period of time. Precipitation is one of the climate variables most difficult to estimate because of its heterogeneous distribution in space and high variability in time (Herold et al., 2015). It is also susceptible to measurement errors caused by wind, evaporation, wetting, splashing and drifting effects, and human errors, such as uncalibrated gauge equipment, acquisition, and data communication problems (Michelson, 2004). Therefore, it is a major challenge to produce consistent precipitation products in space and time over large areas and long periods, especially if such products should be continuously used in real-time operations in hydrology (Golding, 2009; Kucera et al., 2013; Pozzi et al., 2013; Serrat-Capdevila et al., 2013; Verkade et al., 2013; Lettenmaier et al., 2015; Van Osnabrugge et al., 2017).

The main sources of precipitation data are ground-based gauges, weather radars, and satellite instruments (Gilewski and Nawalany, 2018). The first two sources mentioned are more accurate, but they are not uniformly available over large areas such as South America. Satellite data emerge as a potential source of precipitation information in this context, given their capacity to cover large areas and provide continuous space-time data. They are however less accurate and need to be bias corrected (Cassalho et al., 2020). The main sensors used to estimate precipitation are passive microwave, calibrated infrared, and a combination of them (Hong et al., 2018). With the evolution of sensors, active microwave sensors have been added to the satellites over time, such as the Ku-band Cloud Profiling Radar (DPR) on the TRMM Satellite (Simpson et al., 1988), the W-band Cloud Profiling Radar on the CloudSat (Y. Chen et al., 2008; M. Chen et al., 2008b), and Ku-/Ka-band Dual-Frequency Precipitation Radar (DPR) on the GPM satellites (Huffman et al., 2017). Several algorithms have been developed to extract precipitation information from this constellation of satellites, ranging from the simplest IR-based GOES Precipitation Index (GPI) (Arkin and Meisner, 1987) to the most recent and sophisticated NASA GPM (Global Precipitation Measurements) Integrated Multi-satellite Retrievals (IMERGE) (Huffman et al., 2017).

On a global scale, gridded precipitation products have been available since the late 1990 s (Huffman et al., 1997; Adler et al., 2003; Sun et al., 2017; Beck et al., 2017). However, only a few are produced in near real-time, such as the CPC Unified Gauge-Based Analysis of Global Daily Precipitation from the U.S. National Oceanic and Atmospheric Administration (NOAA) (Y. Chen et al., 2008; M. Chen et al., 2008), and the IMERG for GPM dataset from the U.S. National Aeronautics and Space Administration (NASA) (Huffman et al., 2017), which is the successor of the Tropical Rainfall Measuring Mission (TRMM) data products. For South America, the TRMM-MERGE product was developed by the Brazilian Centre for Weather Forecast and Climatic Studies (Centro de Previsão de Tempo e Estudos Climáticos, CPTEC) and made available for near real-time applications (Rozante et al., 2010). It combines gauging station datasets from the Global Telecommunications System, automatic stations from various agencies in South America, and the near real-time TRMM precipitation product to provide a gridded dataset of daily precipitation at 0.25° of spatial resolution for operational applications. When TRMM was discontinued, the product GPM-MERGE was built with the GPM dataset based on the IMERG-E algorithm (the substitute of TMPA-V7 in the TRMM mission). It maintains the same gauge stations and the algorithm MERGE (Rozante et al., 2010), although it presents a higher spatial resolution of 0.1° (Rozante et al., 2018, 2020).

When different precipitation products are available over an area, the question arises whether it would be better to select one product or combine different products. Beck et al. (2017) investigated 22 gridded global and tropical precipitation datasets and concluded that the product that merged all information available, the Multi-Source Weighted-Ensemble Precipitation (MSWEPv1.0), had better overall performance. Recently, Reis et al. (2019) carried out a study comparing the CPC-NOAA and TRMM-MERGE real-time precipitation datasets over 41 river basins, mostly located in Brazil. The authors found considerable differences in space and time between these two datasets, with a tendency to increase differences when moving from south to north and from east to west. For the majority of the studied river basins, the recent decade of data (2008–2017) presented the biggest differences in terms of areal precipitation over the river basins. The authors also highlighted the fact that the differences between the precipitation datasets were propagated, and often amplified in simulated streamflow when used to force a hydrological rainfall-runoff model.

Hydrological data and models can be useful tools for analyzing precipitation datasets. By comparing simulated and observed streamflows, the quality of a precipitation dataset used as forcing for the model can be indirectly assessed and the uncertainties evaluated. This strategy has been used in numerous previous studies to evaluate the quality of precipitation datasets at regional or global scales (e.g., Su et al., 2008; Collischonn et al., 2008; Voisin et al., 2008; Bitew et al., 2012; Li et al., 2013; Falck et al., 2015; Tang et al., 2016; Beck et al., 2017; Hong et al., 2021). Overall, the studies indicate that, once there are better estimates of observed flow than precipitation, the use of hydrological modeling can help in validating the precipitation data. Direct empirical comparisons between rainfall and streamflow can be useful to evaluate rainfall datasets across multiple scales, but also to identify and quantify the magnitude of the uncertainty in the datasets used in hydrological modeling (Levy et al., 2017). Based on the water balance equation, and assuming that a catchment hydrologically behaves like a reservoir system, it is possible to invert the reservoir model equation and express the rainfall as a function of the streamflow and then use this relationship to estimate the uncertainty of the rainfall data (Kirchner, 2009; Henn, 2015).

Hydrological models can also be used to define and evaluate the best combination of multiple precipitation data sources. The MSWEP product is an example of a combined product that uses river discharge observations from stations across the globe and hydrological simulations to correct systematic terrestrial precipitation biases (Beck et al., 2017). It is a fully global, historic precipitation dataset available since 1979 (http://www.gloh2o.org/mswep/). It is based on data from gauge stations, satellite remote sensing, and atmospheric model reanalysis. The hydrological model used to evaluate the performance of the MSWEP product and compare it with other state-of-the-art gauge-adjusted datasets (i.e., WFDEI-CRU, GPCP-1DD, TMPA 3B42, and CPC Unified) was the HBV model (Bergström, 1995). Flow simulations using MSWEP showed better performance (median Nash–Sutcliffe efficiency -NSE of 0.52) than simulations with the other precipitation datasets (NSE values of 0.29–0.39). The median correlation obtained when using the MWSEP product was the best correlation for 60 % of independent precipitation gauges from FLUXNET tower stations used for validation (for more details, see Beck et al., 2017). Recently, Siqueira et al. (2018) applied the MSWEP v1.1 precipitation product with the distributed MGB hydrological model over South America to simulate streamflows. They reported good overall performance of the simulations, with NSE > 0.6 in 55 % of the flow stations. The performance was better in large rivers and wet regions, decreasing in drier climates, where timing errors in rivers with floodplain effects had been reported. To merge different precipitation products in a unique product, Wong et al. (2021) propose a methodological framework that relies on the streamflow response to precipitation. It uses a hydrological model to identify locally, at the (sub-)sub-basin scale, the best product among several gridded precipitation products (satellite-derived and model reanalysis product). The authors use precipitation-gauge stations available to first evaluate the quality of each precipitation dataset and to assess the overall performance of the hydrological model in each streamflow station. The best product is locally selected according to the performance of the hydrological simulations evaluated at discharge gauging locations. The Canadian hydrologic-land surface model H-LSM MESH was used to generate a composite precipitation dataset in the Saskatchewan River basin in Canada, which was then validated by assessing hydrological fluxes and storage at downstream gauge stations.

In many parts of the world, precipitation ground data are not available, or networks are too scarce to be used in the validation of gridded precipitation products. Reliable and consistent long time series of spatially distributed precipitation over large areas are however needed for many applications, including climatological assessments and seasonal streamflow forecasting. They are used to calibrate the hydrological models, warmup the flow forecasting models, bias correct numerical weather forecasts and apply the ensemble streamflow prediction (ESP) method, which relies on historic precipitation and temperature data as future possible climate scenarios (Crochemore et al., 2016; Bennett et al., 2017; Arnal et al., 2017; Harrigan et al., 2018). In flow forecasting applications, these datasets also must be available in real-time or near real-time to allow operational decision making. In Brazil, gridded large-scale precipitation products are of particular importance to the real-time operations of the hydropower sector (Schwanenberg et al., 2015; Gibertoni et al., 2017). The anticipation of hydrological conditions can strongly influence the centralized operation of the electrical system and energy prices (ONS, 2016). Given this regional context, this paper aims to present a methodology that uses a hydrological model and observed discharge time series to quantify uncertainties from the TRMM-MERGE and CPC precipitation datasets, combine

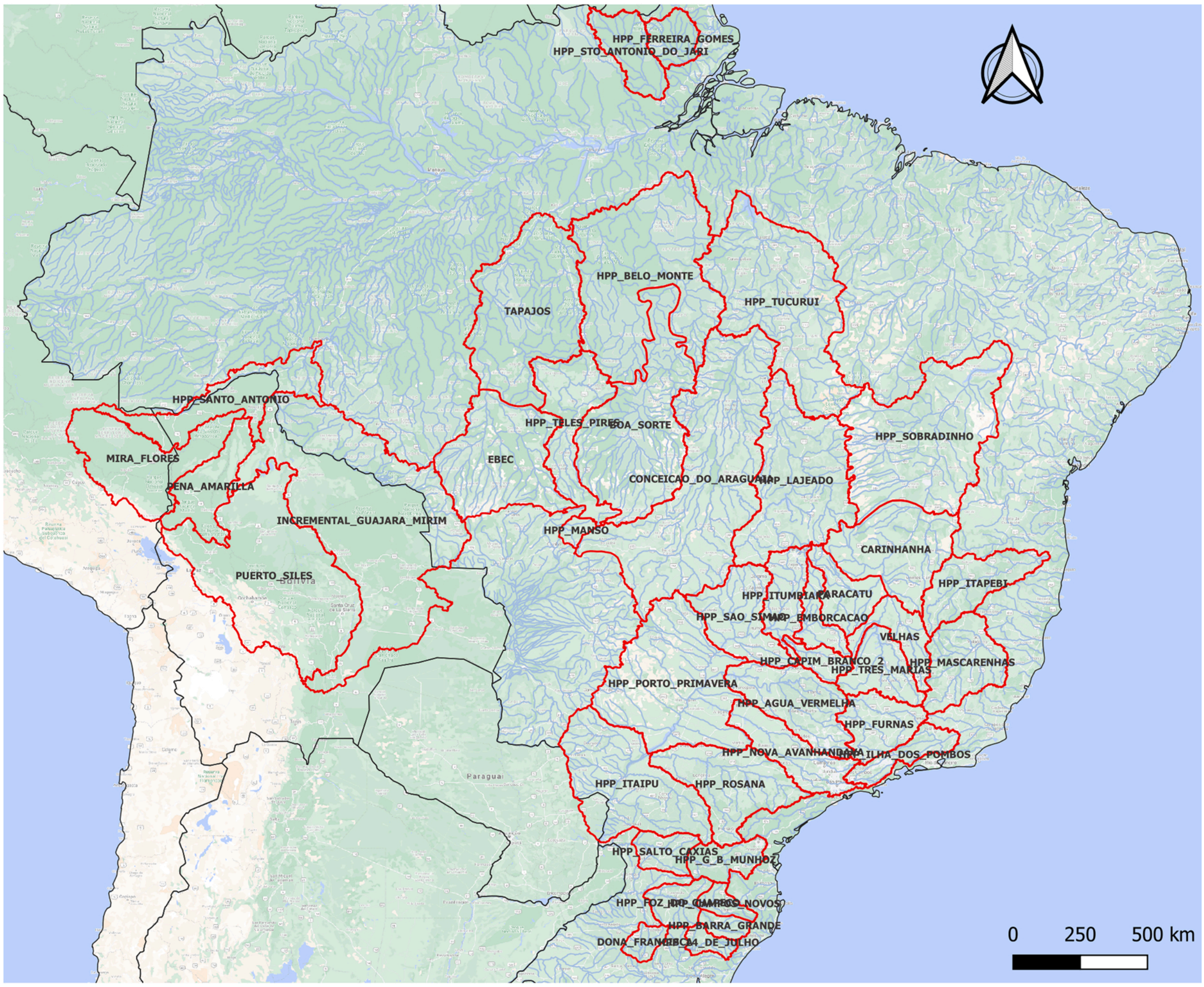

Fig. 1. Geographic location of the study area with the 41 river basins (red contours).

Table 1
Summary of the characteristics of the gridded precipitation datasets as used in this study.

Dataset	Spatial resolution	Time resolution	Time period covered	Data provider and URL for download	Main references
TRMM-MERGE	0.25°	Daily	1997–2017	CPTEC ftp:ftp1.cptec.inpe.br/modelos/io/produtos/MERGETRMM-MERGE/ (data downloaded in 2018; now redirects to GPM-MERGE dataset: http://ftp.cptec.inpe.br/modelos/tempo/MERGE/GPM/DAILY/	Rozante et al. (2010)
CPC	0.5°	Daily	1979–2017	NCEP/NOAA ftp://ftp.cpc.ncep.noaa.gov/precip/CPC_UNI_PRCP/GAUGE_GLB	M. Chen et al. (2008); Y. Chen et al. (2008)
MSWEP	0.1°	Daily	1979–2014	GloH2O http://www.gloh2o.org/mswep/	Beck et al. (2017)

the datasets, and derive a unique precipitation dataset that can be used in (near)real-time applications. The novelty of our approach lies on using both observed and simulated discharge data at the outlet of the river basins to take advantage of the information contained in each precipitation product and derive a unique dataset. Observed discharges are used to quantify precipitation uncertainties and to weight the blending, while discharges obtained from hydrological modeling are used to validate the final precipitation product. Therefore, instead of using a reference (ground or remote sensed) precipitation dataset, which might also contain errors in the precipitation estimates, we use the discharges at the river basin outlets as an independent and more robust reference for hydrological applications at the catchment scale. In addition, this paper presents the validation of the methodology over a large set of catchments (41 river basins), covering a large area of South America.

This paper addresses the following questions: i) How can we use hydrological data and hydrological modeling to blend different observed precipitation datasets and validate the combined product in order to have better precipitation data for hydrological simulation and flow forecasting? ii) How can we extend the combined precipitation product over a period other than the common period of the different observed precipitation time series to foster its use in (near)real-time applications?

This paper illustrates how we can use hydrological data and modeling as a tool to quantify the uncertainty of precipitation estimates, combine different datasets and validate the combined product with the final goal of obtaining a precipitation product relevant to (near)real-time hydrological applications. Our methodology is applied to a large set of 41 river basins that are relevant to the hydropower sector in Brazil and neighboring countries. The TRMM-MERGE and CPC precipitation datasets are used to generate a combined precipitation product. The dataset obtained is compared with the benchmark MSWEP and evaluated in terms of how hydrological simulations compare with observed discharges. In Section 2, the methodology and data used are presented. In Section 3, the results obtained are provided. Section 4 is a discussion of the results, and the conclusions and planned future studies are presented in Section 5.

2. Materials and methods

2.1. Study area and data

The study area comprises 41 river basins distributed in different climatic regions within Brazil and neighboring countries (Fig. 1). The river basins vary in size, with areas ranging from 9300 to 382,000 km^2. The study area extends from the north (Jari River, Madeira River, Xingu River, Tapajos River, Tocantins River, and others) to the south of Brazil (Iguaçu River, Uruguay River, and others) and includes river basins located in the central part of the country (Paraná River, Grande River, São Francisco River, etc.). The 41 river basins provide inflow to 30 hydropower plants (HPPs).

For each river basin, daily areal precipitation was obtained from the TRMM-MERGE, the CPC-NOAA, and the MSWEP datasets (Table 1). Daily areal precipitation time series were calculated using the shape file of the basins and averaging all grid data points falling inside each river basin considered.

Daily discharge data were obtained from the ONS (National Operator of the Electric System; downloaded from https://sintegre.ons.org.br). They correspond to the official HPP natural flow time series and are compiled annually by the national operator. In some cases, it is the ONS that takes into account the regularization effects of the reservoirs and adds their evaporation as well as any water uses to obtain the natural flows of the reservoir. In these cases, the flows are also validated by the electricity generators involved in the process (for more details, see ONS, 2005). Data availability depends on each river basin. For this study, the discharge dataset used covers the period 1979–2018 for all studied river basins.

2.2. Methodological steps

To select a better real-time precipitation dataset among the two available independent data sources and a dataset that is a combination of the two, and to validate the selection and blending procedure using a hydrological model and observed streamflow, an experiment was designed with six basic methodological steps.

Step 1: For each river basin, the daily areal precipitation time series (average over the area of the river basin) is estimated for each precipitation data source. The daily observed flow data are extracted for the same period at each basin. In addition, the total annual precipitation, and the annual mean of observed daily flows are calculated to perform the analysis based on the water balance relationship (Step 2).

Step 2: The uncertainty of each precipitation data source is identified and quantified by using empirical functions that relate the total annual precipitation amounts and the observed annual mean flows. The weights used to build the combined daily precipitation dataset are obtained based on the uncertainty quantified from the annual water balance, as detailed in Section 2.3.

Step 3: Since the two independent precipitation data sources cover different time periods, a procedure is used to extend the combined precipitation dataset over the longest period using the double-mass curve, as described in Section 2.4.

Step 4: For each daily precipitation dataset (the two independent sets and the combined one), the hydrological model is calibrated at each river basin by first applying the traditional split-sample test, which divides the time series (October 1998 to September 2017) into two periods for calibration and validation. This allows to assess the robustness of the model when simulating streamflows over a period independent of the calibration period. We also apply the calibration procedure over the entire data period to evaluate how the parameters of the model change with the length of the time period used for calibration. This step is detailed in Section 2.5.

Step 5: For each precipitation dataset and river basin, the daily flows simulated by the hydrological model (with parameters calibrated over the entire data period) are evaluated against the observed flows at the outlet of the basin. We use a variety of performance metrics, as described in Section 2.6.

Step 6: The extended combined precipitation dataset is evaluated against a benchmark of observed precipitation, and simulated discharges using the new dataset are evaluated against observed discharges.

2.3. Combining two precipitation data sources using the annual water balance

The water balance equation is used in hydrology to describe the flow of water in and out of a system. The period used to calculate the water balance is usually the hydrological year, which is a 12-month period that starts at the end of the dry season. For any given year, the water balance in a river basin with no external inflows from neighboring catchments can be written as:

$$\Delta S = P_i - Q - ET \tag{1}$$

where P_i is the annual precipitation for the given year (total precipitation over the hydrological year) of the precipitation data source i, Q is the annual mean flow, ET is the annual evapotranspiration, and ΔS is the annual variation of storage in the river basin, with all variables expressed in millimeters.

For long-term averages (here calculated over the hydrological year), the change in storage ΔS for an annual time step is marginal and can be considered equal to zero (Shao et al., 2012; Beck et al., 2020). The ET term depends on physical factors, such as the vegetation type, soil cover and land use, as well as on climate factors, such as temperature, solar radiation, humidity, and wind speed, as considered in the Penman-Monteith method used to calculate evapotranspiration (Allen et al., 1998). Therefore, this term can be considered independent of the precipitation data source that is used in Eq. (1). In our study, we are not trying to evaluate the different components of the hydrological balance, but instead we want to capture how the uncertainty varies when we consider different precipitation sources in the same river basin. Eq. (1) can then be simplified, and the precipitation can be written as a function of the flow and the error term that will translate the uncertainties:

$$P_i = f(Q) + \varepsilon_i \tag{2}$$

where $f(Q)$ is the empirical function between the annual precipitation (in millimeters) and the annual flow (in millimeters), and ε_i is the annual error associated with the precipitation source P_i.

The error ε_i is evaluated for each given year using the empirical function that relates each annual precipitation P_i to the annual flow Q. The evaluation is based on the standard deviation of the errors of each precipitation source P_i, and is computed over the time series of annual errors. The standard deviation estimates obtained were used to weight the proportion of each precipitation data source to create a combined precipitation dataset. The weights were based on the proportion of the standard deviation of the errors of one source with respect to the sum of standard deviations of the errors of both sources. The weights were obtained from the following equations:

$$W_j = 1 - \frac{\sigma\varepsilon_j}{\sigma\varepsilon_j + \sigma\varepsilon_k} \tag{3}$$

$$W_k = 1 - W_j \tag{4}$$

where W_j is the weight of the precipitation data source $P_{i=j}$, W_k is the weight of the precipitation data source $P_{i=k}$, $\sigma\varepsilon_j$ is the standard deviation of the annual errors of $P_{i=j}$, and $\sigma\varepsilon_k$ is the standard deviation of the annual errors of source $P_{i=k}$, at each basin.

The main idea behind this methodology is not to identify the precipitation data source that displays the best correlation between P_i and Q. The goal is to access the uncertainty of each source to make it possible to give a higher weight to the source with smaller uncertainty when the two sources of precipitation data are combined in one unique dataset.

Once the weights of each precipitation data source are obtained, they are applied to the daily precipitation time series to generate the combined daily precipitation dataset at each basin, according to Eq. (5):

$$DP_{WC} = DP_j.W_j + DP_k.W_k \tag{5}$$

where DP_{WC} is the daily precipitation of the weighted combination of the two precipitation data sources, DP_j and DP_k.

2.4. Double-mass curve method to extend the combined precipitation dataset

Once the combined precipitation method is applied to the two different precipitation data sources, a combined precipitation dataset for the same period of the shorter precipitation data source is obtained. It is thus necessary to extend, in a consistent way, this combined precipitation time series to also cover the period of the longer available data source. In this study, the double-mass curve method developed by the US Geological Survey was used (Searcy et al., 1960). The method is commonly used in data analyses to check the consistency of hydrometeorological data and adjust the data for any inconsistencies. It is based on comparing the time series of accumulated values at a single data station (or a given data source) with those given by data from other stations in a surrounding area (or other data sources) during the same period. The theory of the double-mass curve is based on the fact that a graph of the accumulation of one time series against the accumulation of another time series, during the same period, plots as a straight line as long as the data are proportional; the slope of the line represents the constant of proportionality (b) between them. Applied to this study, it gives Eq. (6):

$$P_c = \quad P_k.b \tag{6}$$

where P_c represents the precipitation variable of the combined precipitation dataset, and P_k is the precipitation variable coming from the longer time series of the two sources of precipitation used to produce the combined dataset. A break in the slope of Eq. (6) indicates a change in the constant of proportion and the presence of inconsistencies.

In this study, the double-mass curve was applied to annual values of total precipitation as follows.

- For each river basin, for the common period of TRMM-MERGE and CPC-NOAA data (i.e., 1998–2017), the graph of accumulated annual values of the combined dataset is plotted against the graph of the CPC-NOAA dataset, which is the longer precipitation dataset.
- The years with a wide discrepancy around the normal tendency are removed, with the objective of having the most representative parameter to extend the time series.
- The constant of proportionality obtained with this correlation is used to multiply the past period of the longer data source, obtaining thus a complete time series of daily precipitation back until 1979, in order to represent the extension of the combined precipitation dataset.

To compare the combined precipitation dataset with the benchmark precipitation (MSWEP dataset), and to evaluate how the dispersion of the error varies in time, the standard deviation of the annual precipitation errors (observed precipitation minus the value calculated with the empirical functions of Eq. (2)) were calculated for 1980–2014 (full hydrological years of the benchmark data available) in a five-year moving window. To improve the analysis and avoid scale distortions caused by differences in wetter or drier years between MSWEP and the combined precipitation dataset, the standard deviation error was normalized by dividing its value by the average precipitation of each five-year window.

2.5. HEC-HMS hydrological modeling and flow analyses

To validate the combined precipitation dataset obtained, a hydrological model was used to evaluate the accuracy of the simulated discharges when this dataset drives the model. The hydrological model used in this study is the one proposed in the suite of the HEC-HMS model (Feldman, 2000). It is a flexible and user-friendly suite of models that can be used for many hydrological applications, such as urban and rural flooding, flood warning systems, water uses planning, etc. The models can be applied to simulate a single flow event or to perform continuous hydrological simulations in a semi-distributed modeling configuration. The modules can be chosen according to the needs of the user, the application envisaged and the expected accuracy (Feldman, 2000; Najim, 2013). Users can, for instance, select specific modules of the loss method, the transformation method, and the base flow method (Scharffenberg, 2016).

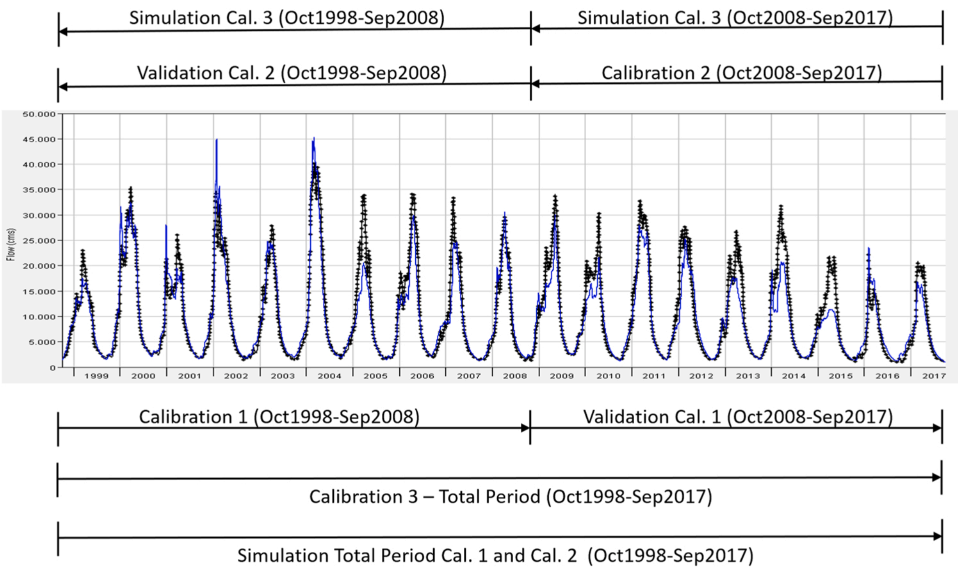

Fig. 2. Illustration of the split-sample approach applied to evaluate the hydrological model: two periods of 10 years each are used for calibration/validation (Cal. 1 and Cal. 2); the total period is used for calibration (Calibration 3), and for comparison with the results of the two separated periods (Simulation Cal. 3), and the results of the two separated validation periods (Simulation Total Period Cal. 1 and Cal. 2). The blue (black) hydrograph illustrates the simulated (observed) flow for a given river basin.

In this study, the HEC-HMS modeling framework was run for continuous simulations at the daily time step. The interception was modeled using the simple canopy (Bennett, 1998) and the simple surface (Bennett, 1998) methods. The excess of precipitation arrives on the soil and is captured until the storage capacity of the surface is filled and then runoff starts. The water in the surface will then infiltrate into the soil. The soil moisture accounting method is the unique module in the framework able to run a continuous simulation. It uses three layers to represent the dynamics of the water movement in the soil. For a given precipitation and evapotranspiration, it computes the basin's surface runoff, groundwater flow, losses, and the deep percolation over the entire basin (Bennett, 1998). The Clark unit hydrograph was used to incorporate the translation of runoff through time within the basin and the attenuation of runoff through storage in a linear reservoir. Its principal parameters are the time of concentration, defining the travel time in the sub-basin, and the storage coefficient (Kull and Feldman, 1998). The linear reservoir method (Kull and Feldman, 1998) was used to represent the base flow. It uses a linear reservoir to model the recession of the base flow after a storm event, using the principles of conservation of mass. The lateral outflow of the groundwater is connected with the infiltration from the soil moisture accounting loss method. For the routing, the Lag method or the Muskingum-Cunge Routing method were used, depending on the complexity of the basin and the extension of the river reach.

The split-sample approach (Klemes, 1986) was used to calibrate the hydrological model and test its robustness (validation). Each time series is split into two and both parts are used for calibration and validation. The results in terms of model performance are evaluated for the two validation periods and compared with the performance results obtained over the same periods but with the calibration based on the complete period. The main objective of these various calibration and validation periods is to verify that the calibration of the total period, which is used in the next steps, is robust and has equivalent performance to that of the split-sample approach. Fig. 2 illustrates the approach used and the different calibration and validation periods of the HEC-HMS hydrological model.

The model was calibrated using a daily time step and for each source of precipitation separately. Large basins with different climatic characteristics across space were divided in sub-basins to better capture differences in precipitation and produce a better rainfall-runoff transformation. In total, there are 26 parameters to be calibrated in the HEC-HMS model. The parameters that have a stronger influence on the model outputs are the time of concentration and the storage coefficient, which are linked to the Clark unit hydrograph module, the maximum infiltration rate, the soil total storage, the soil tension storage, and the maximum soil percolation rate, which are linked to the loss module. An initial manual calibration was performed to obtain the first parameters set. Then, the automatic calibration procedure, available in the HEC-HMS model, was applied to obtain the optimal parameters using the Univariate-Gradient Search Algorithm. The objective function used for the Clark unit hydrograph parameters was the Minimum of Peak-Weighted RMS Error and, for the loss parameters, the Minimum Sum of Squared Residuals (Diskin and Simon, 1977). Since the objective functions are more sensitive to the volumes and peaks of the hydrographs, it is sometimes necessary to adjust the base flow parameters to have a better fit of the recession of the hydrographs, after running the model optimization. The calibration process is repeated three times for each calibration period (Fig. 2), for each precipitation data source and for the combined precipitation dataset, and for each river basin.

2.6. Evaluation metrics

To analyze the performance of the hydrological models run in this study (HEC-HMS model calibrated with the different observed precipitation datasets), the Nash–Sutcliffe efficiency - NSE (Nash, 1970), the Kling–Gupta efficiency - KGE (Gupta et al., 2009), the Mean Absolute Error - MAE, and the R^2 (coefficient of determination) were used as performance indicators. These metrics are used to compare the daily simulated flows with the daily observed flows. They were evaluated for the calibration-independent time periods defined in Fig. 2 (October 1998 to September 2008; October 2008 to September 2017). In our evaluation, the performance indicators obtained for the validation periods 1 and 2 were used to evaluate the performance of the hydrological model at each river basin. The performance obtained during the total calibration period was used to define the best precipitation data source for each river basin.

NSE: measures how good the results of the model are compared with the mean observed discharge. Values equal to 1 indicate a perfect fit, and values smaller than zero indicate that the mean discharge is a better predictor than the hydrological model.

$$NSE = 1 - \frac{\sum_{i=1}^{n}\left(Y_i^{sim} - Y_i^{obs}\right)^2}{\sum_{i=1}^{n}\left(Y_i^{obs} - \overline{Y}^{obs}\right)^2} \tag{7}$$

where Y_i^{sim} is the simulated value at time step i, Y_i^{obs} is the observed value at time step i, $\overline{Y}^{obs}$ is the mean of the observed value, and n is the number of time steps.

KGE: provides a decomposition of the Nash–Sutcliffe efficiency analysis. Values close to 1 indicate a more accurate model.

$$KGE = 1 - \sqrt{(r-1)^2 + \left(\frac{\mu_{sim}}{\mu_{obs}} - 1\right)^2 + \left(\frac{\sigma_{sim}}{\sigma_{obs}} - 1\right)^2} \tag{8}$$

where, in the first part, r is the linear correlation between simulations and observations. In the second part (a measure of error variability), μ_{sim} is the mean of the simulations Y_i^{sim}, and μ_{obs} the mean of the observations Y_i^{obs}. In the third part (a bias term), σ_{sim} is the standard deviation of the simulations, and σ_{obs} is the standard deviation of the observations.

MAE: gives the average deviation between the simulated and the observed discharges. Values closer to zero indicate better performance.

$$MAE = \frac{1}{n}\sum_{i=1}^{n}\left|Y_i^{sim} - Y_i^{obs}\right| \tag{9}$$

where definitions are the same as in Eq. (7).

R^2: is the proportion of the variance in the dependent variable that is predictable from the independent variable. A value close to 1 indicates a better fit of simulations to observations.

$$R^2 = \frac{\sum_{i=1}^{n}\left(Y_i^{sim} - \overline{Y}^{obs}\right)^2}{\sum_{i=1}^{n}\left(Y_i^{obs} - \overline{Y}^{obs}\right)^2} \tag{10}$$

where definitions are the same as in Eq. (7).

3. Results

3.1. Standard deviation of the annual precipitation errors

Fig. 3 shows the boxplot distribution of the standard deviation of the annual precipitation errors (ε_i from Eq. (2)) obtained from the two sources of precipitation data and the combined precipitation dataset. The standard deviation values were evaluated over all 41 river basins and 19 years of data (October 1998 - September 2017), and the linear function was the best fit in all basins, which makes sense since the annual water balance was represented by a linear function in Eq. (1). The standard deviation of annual precipitation errors from the benchmark MSWEP dataset, for all river basins and the period from 1998 to 2017, is also shown as reference. Table 2 shows the results for each river basin, as well as the weights applied when combining the two precipitation data sources.

The dispersion of the annual precipitation errors is reduced when the different precipitation data sources are combined. The combined precipitation dataset shows a lower standard deviation of the annual precipitation errors than the original datasets on 15 out of 41 river basins, and its boxplot distribution is closer to the reference MSWEP dataset. Although the median value of the error standard deviation is close to the TRMM-MERGE dataset median value, the interquartile range between the 75th and 25th percentiles is smaller in the combined dataset. This measure of dispersion of the precipitation errors around the empirical function gives an idea of the uncertainty of each precipitation dataset. In the combined dataset more weight is given to the precipitation dataset with lower uncertainty. In Table 2, we can see that the TRMM-MERGE dataset has more weight than the CPC dataset in 30 out of 41 river basins, and both have equal weight in 2 river basins.

3.2. Hydrological model performance

The three precipitation datasets (TRMM-MERGE, CPC and Combined) were used to calibrate and validate the HEC-HMS hydrological model in all 41 river basins. Fig. 4 shows the density functions representing the distribution of the four performance metrics analyzed: KGE, NSE, MAE (calculated in terms of specific discharge, in l/s.km^2 to permit comparison of the values in basins with different sizes), and R^2. The values obtained in calibration (validation) are in red (blue). Table 3 shows the median values of the metrics when considering all river basins, calibration, and validation periods (as defined in Fig. 2), and for each precipitation dataset.

For most of the basins, the difference in performance metrics between calibration and validation is less than 10%. The calibrated models can be considered to perform well over the large river basin dataset of this study. For most of the 41 river basins, the NSE and KGE criteria are higher than 0.60, and the R^2 coefficient is higher than 0.55. Table 3 shows that median values of NSE and KGE vary

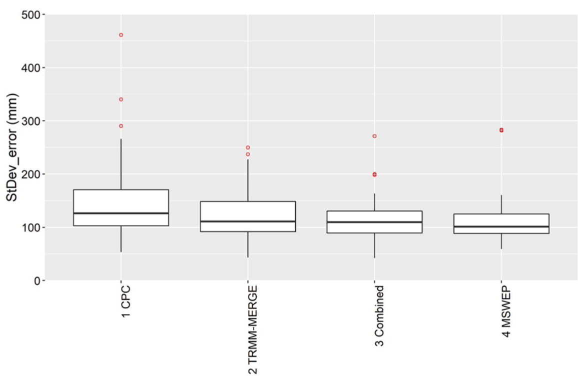

Fig. 3. Box-plot of the standard deviation of the annual precipitation errors (in mm) for areal precipitation over 41 river basins and for each precipitation dataset: CPC, TRMM-MERGE, Combined CPC and TRMM-MERGE and the reference MSWEP.

Table 2
Standard deviation of the annual precipitation errors (in mm) for each river basin and precipitation dataset (TRMM-MERGE, CPC and Combined TRMM-MERGE and CPC) and weights used for the combined precipitation dataset. The dataset with the best performance is colored.

RIVER BASIN	Standard Deviation of annual precipitation errors			Weights used in the combined dataset	
	TRMM-MERGE	CPC	Comb.	TRMM-MERGE	CPC
1) HPP 14_DE_JULHO	128	100	101	**0.44**	**0.56**
2) HPP DONA_FRANCISCA	163	180	163	**0.53**	**0.47**
3) HPP BARRA_GRANDE	196	124	134	**0.39**	**0.61**
4) HPP CAMPOS_NOVOS	141	135	130	**0.49**	**0.51**
5) HPP FOZ_DO_CHAPECO	237	181	198	**0.43**	**0.57**
6) HPP G_B_MUNHOZ	111	161	122	**0.59**	**0.41**
7) HPP SALTO_CAXIAS	149	290	159	**0.66**	**0.34**
8) HPP ITAIPU	115	126	116	**0.52**	**0.48**
9) HPP ROSANA	116	80	75	**0.41**	**0.59**
10) HPP PORTO_PRIMAVERA	95	106	90	**0.53**	**0.47**
11) HPP NOVA_AVANHANDAVA	199	126	138	**0.39**	**0.61**
12) HPP AGUA_VERMELHA	169	101	120	**0.38**	**0.62**
13) HPP FURNAS	85	121	96	**0.59**	**0.41**
14) INC_HPP SAO_SIMAO	99	100	94	**0.50**	**0.50**
15) INC_HPP ITUMBIARA	120	150	124	**0.56**	**0.44**
16) HPP CAPIM_BRANCO_2	93	98	89	**0.51**	**0.49**
17) HPP EMBORCACAO	97	146	110	**0.60**	**0.40**
18) HPP ILHA_DOS_POMBOS	89	115	79	**0.56**	**0.44**
19) HPP MASCARENHAS	85	93	80	**0.52**	**0.48**
20) HPP ITAPEBI	43	54	42	**0.55**	**0.45**
21) HPP TRES_MARIAS	110	153	110	**0.58**	**0.42**
22) VELHAS	92	124	99	**0.57**	**0.43**
23) PARACATU	93	103	89	**0.52**	**0.48**
24) CARINHANHA	95	109	99	**0.54**	**0.46**
25) HPP SOBRADINHO_INC	122	135	127	**0.52**	**0.48**
26) HPP LAJEADO	76	100	72	**0.57**	**0.43**
27) CONC_DO_ARAGUAIA	78	119	70	**0.60**	**0.40**
28) HPP TUCURUI_INC	121	162	125	**0.57**	**0.43**
29) BOA_SORTE	101	227	114	**0.69**	**0.31**
30) HPP BELO_MONTE_INC	135	259	142	**0.66**	**0.34**
31) HPP MANSO	198	266	200	**0.57**	**0.43**
32) HPP TELES_PIRES	87	190	102	**0.69**	**0.31**
33) EBEC	69	171	68	**0.71**	**0.29**
34) HPP TAPAJOS	89	340	106	**0.79**	**0.21**
35) PUERTO_SILES	72	81	73	**0.53**	**0.47**
36) PENA_AMARILLA	152	136	139	**0.47**	**0.53**
37) MIRA_FLORES	148	105	110	**0.41**	**0.59**
38) INC_GUAJARA_MIRIM	93	93	89	**0.50**	**0.50**
39) INC_ HPP_SANTO_ANTONIO	111	131	104	**0.54**	**0.46**
40) HPP STO_ANTONIO_DO_JARI	228	257	137	**0.53**	**0.47**
41) HPP FERREIRA_GOMES	250	461	271	**0.65**	**0.35**

from 0.71 to 0.81 in calibration, and from 0.68 to 0.78 in validation. Median values of R^2 coefficient in calibration and validation are also very close. These results indicate that the model calibration is sufficiently robust to represent the characteristics of the basins in different periods. Fig. 5 also shows that the combined dataset results in a more consistent calibration and validation performance, with sharper curves and fewer outliers of performance. The combined dataset is also the one that presents the highest median values of NSE, KGE and R^2 and the lowest median values of MAE (Table 3). These results can also be another indicator of the robustness and good performance of the combined precipitation dataset.

3.3. Selection of the best precipitation dataset

After the evaluation and validation of the performance of the hydrological model for each river basin, the best performing precipitation dataset was evaluated in terms of simulated discharges. The simulations were made using the model with parameters calibrated with each precipitation dataset and over the entire period (October 1998 - September 2017). Fig. 5 shows the MAE, KGE, NSE, and R^2 performance metrics obtained for the 41 river basins and the three sources of precipitation data (TRMM-MERGE, CPC, and the combined precipitation dataset).

In general, the simulated discharges using the CPC precipitation dataset clearly performed worse for the four indicators analyzed. The simulated discharges using the combined precipitation dataset performs best for almost all basins. When the scores are not the best for this dataset in a river basin, the differences are less than 10 % in the majority of the cases (not shown). The best performance of the combined dataset is clearly shown with the NSE, MAE and R^2 criteria. In terms of the KGE criterion, 50 % of the river basins present values higher than 0.79 when using the combined and the TRMM-MERGE precipitation datasets. There are small differences in KGE between these two datasets, although the use of the combined dataset resulted in fewer outliers in terms of performance and notably

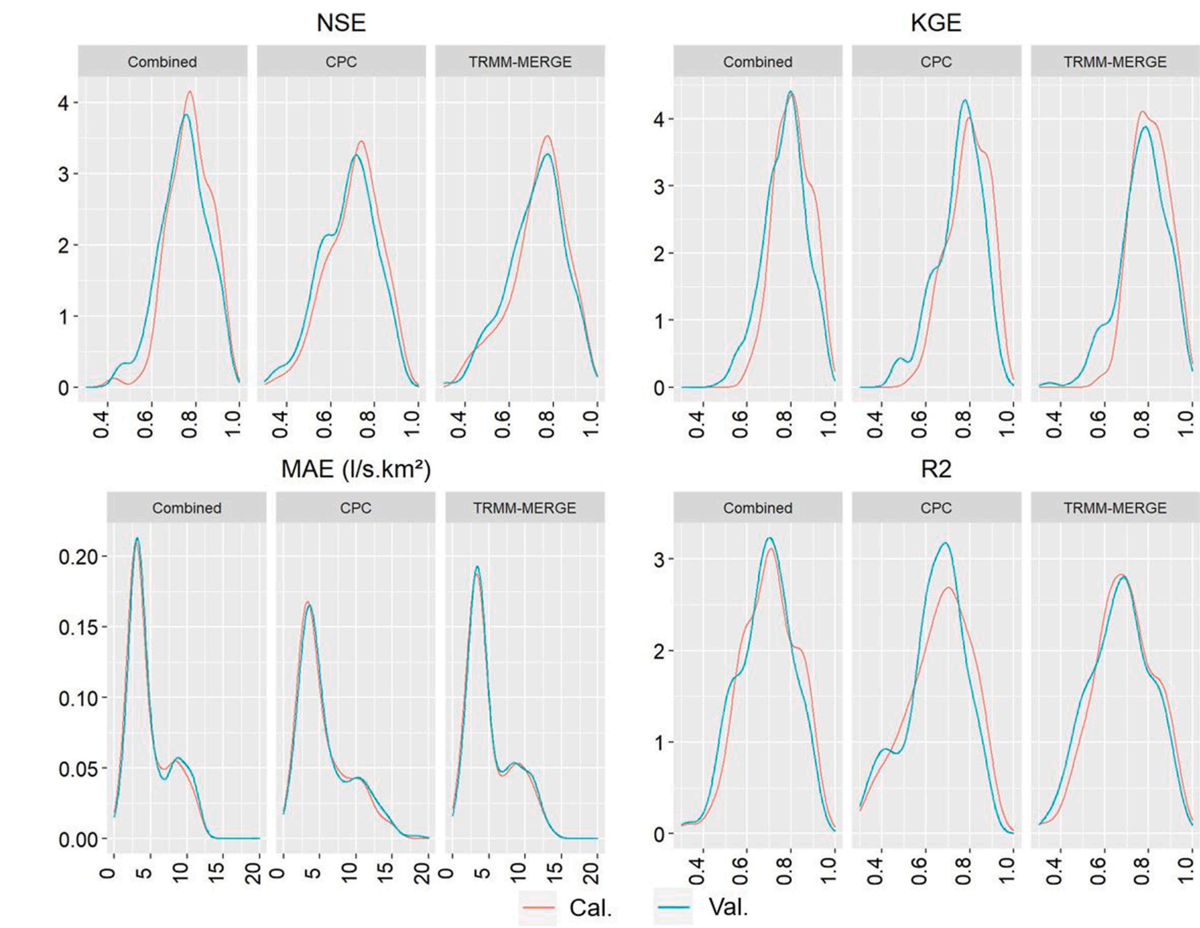

Fig. 4. Density functions of the values of the performance metrics NSE, KGE, MAE and R^2 for the simulated flows in calibration (line in red) and validation (line in blue) periods from the hydrological model HEC-HMS applied over 41 river basins with the TRMM-MERGE, CPC and Combined CPC and TRMM-MERGE precipitation datasets. Calibration and validation periods come from the split-sample test of the total 1998–2017 data period.

Table 3
Median values of the performance metrics NSE, KGE, MAE and R^2 for the simulated flows in calibration and validation periods from the hydrological model HEC-HMS applied over 41 river basins with the TRMM-MERGE, CPC and Combined CPC and TRMM-MERGE precipitation datasets. Calibration and validation periods come from the split-sample test of the total 1998–2017 data period.

Metric		Median values		
		TRMM-MERGE	CPC	Combined
NSE	Calibration	0.73	0.71	0.77
	Validation	0.71	0.68	0.75
KGE	Calibration	0.81	0.79	0.81
	Validation	0.78	0.75	0.78
MAE (l/s.km^2)	Calibration	3.87	4.07	3.45
	Validation	3.94	4.33	3.64
R^2	Calibration	0.69	0.66	0.70
	Validation	0.67	0.64	0.69

less river basins with low values of KGE. For individual river basins showing the lowest values of KGE with the combined dataset, the differences regarding the KGE with the TRMM-MERGE are lower than 8 %.

3.4. Extension of the combined precipitation dataset

Once the evaluation showed that the combined precipitation of the two precipitation data sources achieved the best performance

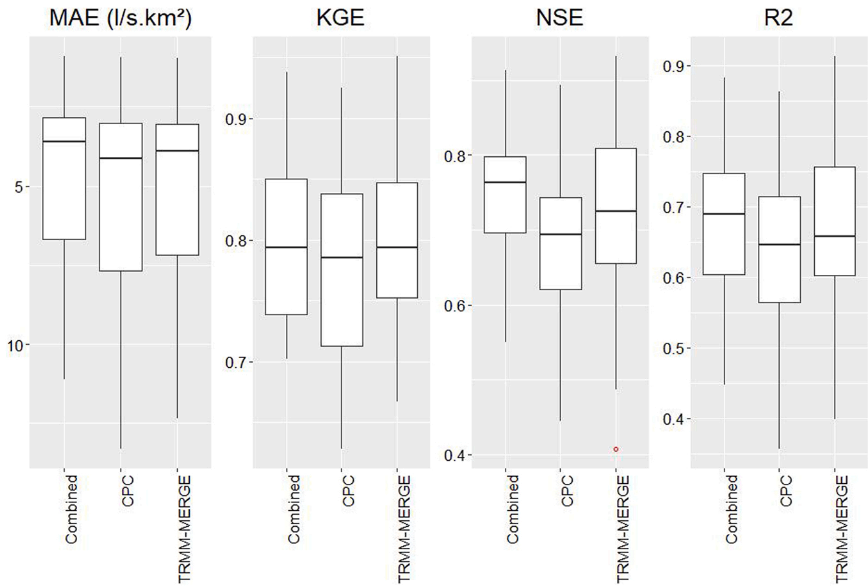

Fig. 5. Performance metrics MAE, KGE, NSE and R^2 for the simulated flows in the calibration period 1998–2017 from the hydrological model HEC-HMS applied over 41 river basins with the TRMM-MERGE, CPC and Combined CPC and TRMM-MERGE precipitation datasets.

over the common period of data (October 1998 - September 2017), the next step was to use the double-mass procedure (Section 2.4) to extend the combined dataset. The correlation of the double-mass curve between the longest dataset (CPC) and the combined dataset was used to extend the period of the combined dataset until 1979 (first year of data available in the longest CPC dataset). To validate the extended dataset obtained, the hydrological models were run for each river basin, with parameters calibrated for the period 1998–2017. The performance of the streamflow simulations of this recent period was compared with the performance of the simulations obtained over the extended (validation) period of 1979–1997. Fig. 6 shows the distribution of streamflow performance metrics (MAE, NSE, and R^2) over the 41 river basins of this study.

In terms of accuracy of the streamflow simulations (MAE), the average error for the extended (validation) period (1979–1998) is slightly lower than the average error of the recent (calibration) period (1998–2017). Considering the NSE criterion, the extended period has, on average, better performance (higher NSE values) than the recent period. For the R^2 correlation, the values obtained over the extended period are clearly higher than the values obtained over the recent period. These results validate the extension of the combined precipitation dataset in terms of its ability to provide streamflow simulations in the extended earlier period that match the observed streamflows as well as in the more recent period of the combined precipitation dataset.

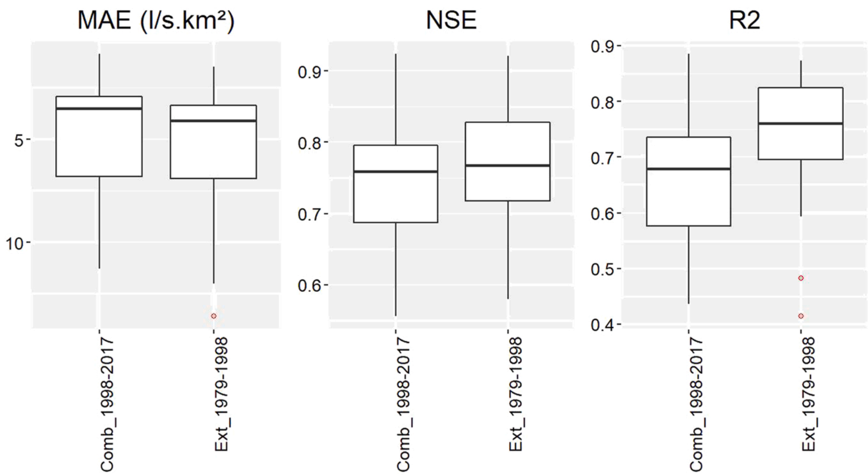

Fig. 6. Performance metrics MAE, NSE and R^2 for the simulated flows from the hydrological model HEC-HMS applied over 41 river basins with the Combined CPC and TRMM-MERGE precipitation datasets in the calibration period 1998–2017 and in the validation extended period 1979–1998.

3.5. Comparison of the combined precipitation dataset with the benchmark

The combined precipitation dataset was evaluated against the benchmark MSWEP dataset. Fig. 7 shows the evolution in time of the normalized standard deviation of the annual precipitation errors obtained for 1980–2017 in a five-year moving window. The thickest lines represent the median of the values for all river basins and the shadowed areas show the 25th and 75th percentiles (variability among river basins).

The extended period of the combined precipitation (before 1998) tends to have a behavior closer to the benchmark. It shows similar standard deviation of annual precipitation errors, but higher values: median values are closer to 6% versus median values closer to 5 % for the benchmark. The combined precipitation dataset does not exhibit a visible temporal trend. However, the standard deviation of the precipitation errors decreases after the year 2000, to increase again just a few years later.

The standard deviation of the MWSEP annual precipitation errors is smaller and more stable over time comparatively to the combined precipitation dataset. It also shows less variability among river basins. After around 1998, there is a reduction in the MSWEP error standard deviation, probably due to the use of satellite observations to improve the estimates of precipitation. After 2008, median values tend to increase again to values similar to those before 1998, although the variability among river basins remain reduced.

When the entire period (1980–2017) is considered, the combined precipitation dataset has a higher median and variability among river basins than the benchmark, but the difference can be considered small, especially considering that the combined precipitation is a real-time dataset, subject to errors that might be corrected afterwards, and the level of consistency is not comparable to a reanalysis dataset such as MSWEP.

In terms of spatial distribution of the errors, there is no evidence of a pattern or regions with a clear higher normalized standard deviation of the errors (not shown). For almost all basins, the combined precipitation dataset displays values between 4 % and 9 %. Only a few basins have values higher than 11 %, and they are not concentrated in the same region.

3.6. Examples of simulated hydrographs using the combined precipitation dataset

As showed in Sections 3.2 and 3.3, the combined precipitation dataset displayed good performance for the period used to build it from the two existing data sources, i.e., 1998–2017, with NSE and KGE values above 0.75. Fig. 8 shows three examples of the simulated flows using the combined precipitation dataset for the complete period generated from this study, i.e., from October 1st, 1979 to September 30th, 2021. Three river basins were selected to represent the southern region (HPP Foz do Chapecó at the Uruguai River), the southeast region (HPP Emborcação at the Paranaíba River), and the north region (HPP Santo Antônio at the Madeira River).

In the southern region, the weather does not present a clear seasonality and peaks of flow may occur in any month of the year. The simulated flows tend to underestimate the highest peaks and overestimate the lowest flows (NSE = 0.78). In the southeast region, seasonality is present, and the wet season is from November to March. The simulated flows tend to overestimate the flow peaks for the period 1983–1993 and underestimate them for 2005–2010. Despite these tendencies, this river basin also presents a good statistical fit, with NSE value of 0.76. In the north region, the biggest basin of our dataset is shown. A clear seasonality is observed, with the wet season from December to May. The simulated flows display an overall better and more stable performance, with a good fit to flow peaks and flow recession periods (NSE = 0.87).

4. Discussion

This study proposes a methodology that allows us to combine, extend and validate two precipitation datasets, based on precipitation gauges and satellite-based products (CPC and TRMM-MERGE), by using observed and simulated discharges at river basin outlets. By relying on discharge data and hydrological modeling to process the global gridded precipitation products, it provides a framework that can be applied, in particular, in large areas where ground networks of rain gauges, often considered as the most

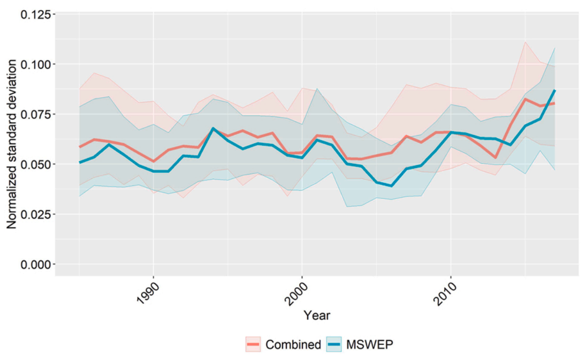

Fig. 7. Normalized standard deviation of the annual precipitation errors with the combined precipitation dataset (red) and the benchmark MSWEP dataset (blue). Median values (lines) and 25th and 75th percentiles (shadowed areas) are calculated in a five-year moving window and over 41 river basins.

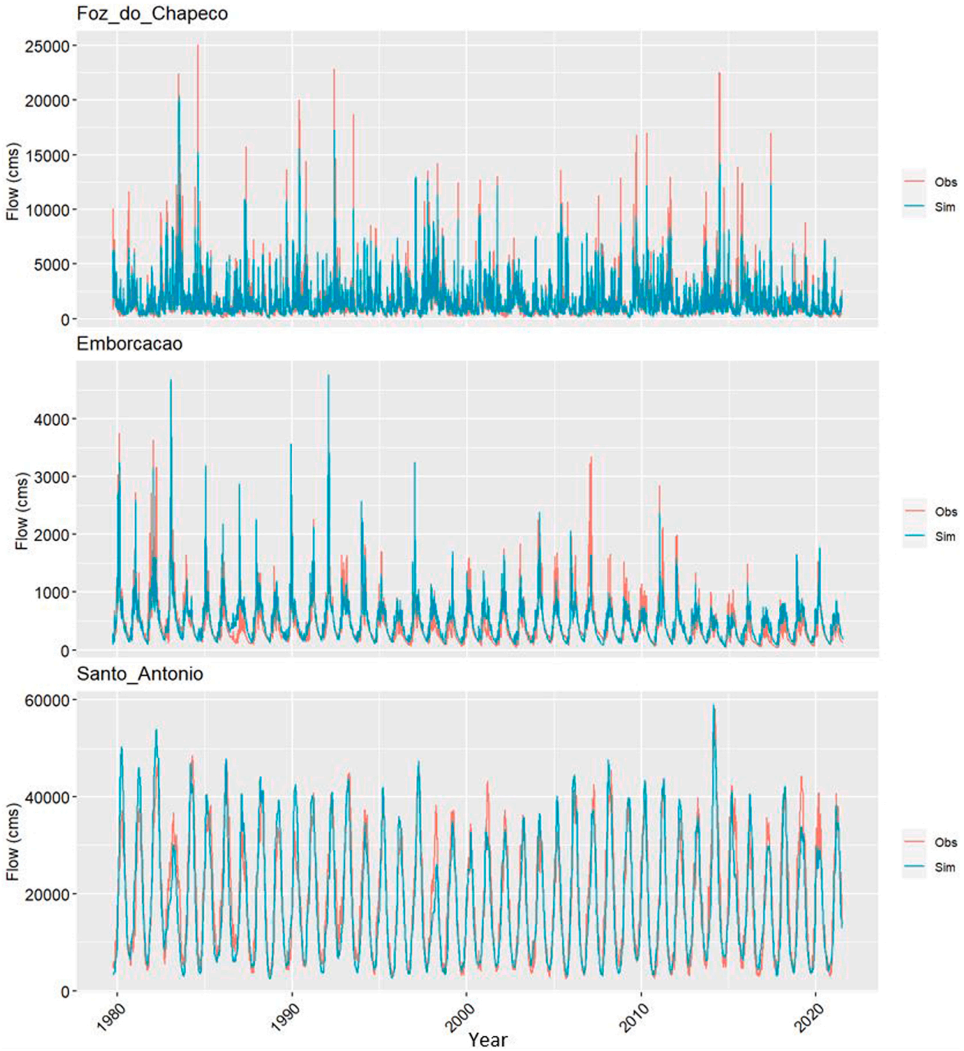

Fig. 8. Simulated (blue) and observed (red) daily streamflows for three representative river basins from October 1st, 1980 to September 30th, 2021: Foz do Chapecó (Uruguai River) in the south region (top panel), Emborcação (Paranaíba River) in the southeast region (middle panel), and Santo Antônio (Madeira River) in the north region (bottom panel).

accurate source of precipitation information, is not reliable or dense enough for hydrological applications. We tested and validated the approach over 41 river basins in Brazil and neighboring countries (basin sizes ranging from 9300 km^2 to 382,000 km^2). This study area has a continental dimension, exhibiting diverse patterns of weather and climate governed by large scale climate phenomena (Garreaud et al., 2009). We find climate regimes with a clear precipitation seasonality: the drier semi-arid weather at the northeast region (Tinôco et al., 2018), the South America monsoon system responsible for high precipitation amounts at the southeast and central-western of Brazil (Ferreira and Gan, 2011), and the intense convective storms from tropical weather at the Amazon region (Garreaud et al., 2009). The study area also comprises a weather type with no seasonality: the subtropical weather at the south region of the continent, which presents wet and dry periods in any month of the year (Garreaud et al., 2009). This large domain of application illustrates the ability of the approach to provide the means to combine precipitation datasets under a variety of hydrological and climatic conditions.

The approach proposed in this study also allow us to take advantage of the quality control and knowledge already developed in each precipitation source, such as the five levels quality control at the CPC dataset (Chen. M, et al., 2008). Observed discharges are used in the computation of the annual water balance in order to quantify the uncertainties of each precipitation source. This is done by using the standard deviation of the errors, which are then used to define the weights that will generate the blending of the different precipitation datasets at each river basin. This first step is an important step before performing any hydrological analysis or using the available datasets in real time flow forecasting (Levy et al., 2017). In our study we found that the uncertainty, as measured by the standard deviation of annual precipitation errors, had the highest values in the CPC dataset for most of the basins. This result agrees with the finds of Rozante et al. (2010), when comparing the performance of TRMM-MERGE product with the gauge based product OBS90, showing a superior quality of the MERGE product over the gauge-based CPC product. When the precipitation data sources were combined, the new dataset displayed remarkably similar annual uncertainty to the one evaluated from the source which had the smallest standard deviation values. However, the uncertainty variability among the river basins was reduced in the combined dataset and became more similar to the one displayed by the reference dataset we used in this study, the non-real time MSWEP precipitation dataset. This result is in line with the results obtained by Beck at al. (2017), where the authors reported the superior quality of their merged product (based on satellite, rain gauges and reanalysis) when the product and the individual sources were evaluated against ground observations of precipitation.

The data source presenting the lower standard deviation of annual precipitation errors is usually the one with the higher weight when combining the daily precipitation data. The proposed method uses the annual uncertainty to define the blending weights but blends the precipitation datasets at a daily time step on the river basin scale. Therefore, the reduction of uncertainty that results from the combination of individual datasets also impacts the quality of the precipitation at shorter time scales. At the annual scale, large errors of each data source were smoothed during the combination process in several cases (15 out of the 41 basins), and the resultant precipitation dataset displayed lower standard deviation of annual precipitation errors. At the daily scales, where the hydrological models are usually calibrated and validated for hydrological applications such as streamflow forecasting and climate change impact assessment, the performance was better for practically all river basins, reflecting lower uncertainty from the combination of precipitation data sources also at this shorter time step. These results are the first indication that the methodology proposed for the combination of the different sources of data can lead to a precipitation forcing dataset that is more robust and display lower uncertainty at different time scales. This is relevant because lower uncertainty can result in better and more robust calibration of the hydrological model, with fewer differences in performance of flow simulations when comparing validation and calibration periods. Robustness in hydrological modeling is crucial for real time flow forecasting, when future events that were not experienced in the past, and hence were not included in the model calibration process, might occur and generate extreme situations of interest for hydrological risk and water resources management.

Parameter estimation and uncertainty analysis in hydrological modeling (see, for instance, Zhang et al., 2016; Teweldebrhan et al, 2018; Herrera et al., 2021) was not in the scope of this study. We assumed that the application of the split sample test and the use of a long time series were satisfactory to achieve robust parameters of the hydrological model. When calibrating the hydrological models, we generated nine simulations, three for each precipitation forcing (TRMM-MERGE, CPC, and their combination). Following the traditional split-sample test, there were two calibration-validation procedures applied each to half of the sample. Additionally, one calibration covered the entire data period of almost twenty years. The results were evaluated using performance indicators (NSE, KGE, MAE, and R^2) and it was shown that, for most of the basins, the results in terms of performance of simulated flows are similar among the different periods. This enabled the use of the hydrological model as a tool for the selection and validation of the precipitation datasets, including the combined precipitation dataset. This can be an interesting strategy when the focus of a precipitation dataset analysis is its specific use for hydrological applications, as, for instance, in seasonal streamflow forecasting, where the traditional method of ESP (Ensemble Streamflow Prediction) for issuing reliable hydrological forecasts requires long series of homogeneous historic precipitation data. Wong et al. (2021) also illustrated the interest of evaluating precipitation products in terms of streamflow simulations. They showed that, at the scale of a large river basin in Canada, the best precipitation product evaluated against the precipitation-gauge stations did not necessarily display the best streamflow performance across the sub-catchments of the river basin. The authors also highlighted the benefit of using streamflow as it presents smaller uncertainties when compared to other hydrological information that can be derived from a hydrological model.

Our results are also in agreement with the conclusions drawn by Beck et al. (2017, 2019), which evaluated a large group of observed precipitation data sources and concluded that the combination of data sources into one reanalysis dataset provided better estimates of precipitation. The unique MSWEP (Multi-Source Weighted-Ensemble Precipitation) dataset of global terrestrial precipitation dataset provides a high-resolution (3-hourly temporal and 0.1° spatial resolution) reanalysis dataset. While it was used in our study as a reference dataset to evaluate (and validate) the combined dataset built, its direct use for real time operations is not possible given the fact that this dataset it is not yet processed to be available in real time. Combined precipitation datasets are particularly useful when water managers have to operate over large areas, from tens to hundred square kilometers, and cannot compile different data sets in real time for each river basin under their management. The use of a unique and robust precipitation dataset is an asset in operational settings and continental-wide applications. The fact that our combined dataset performs well compared with the MSWEP dataset also opens the opportunity for the future use of the MSWEP dataset when it will become available in real time.

The performance results of this study can be compared with other large-scale model experiments in terms of overall performance. For the NSE criterion, our results show the performance is higher than 0.60 for 97 % of the basins and the average NSE over the study area is 0.75. The KGE criterion is also higher than 0.60 for all basins and the average value is 0.77. The average coefficient of correlation is 0.67 for the study basins. Siqueira et al. (2018), using a distributed hydrological model (MGB) and the MSWEP data from Beck et al. (2017) as precipitation forcing, obtained NSE values for discharge and water levels higher than 0.60 for 55 % of the studied cases and KGE values higher than 0.60 in 70 % of the studied cases of streamflow simulation. According to the authors, the global models (WaterGap, LISFLOOD, and HTESSEL/CaMaFlood) showed more than 40 % of the basins in South America with an NSE and a KGE lower than zero. When comparing the HEC-HMS models calibrated in this study with the other experiments realized in South America, we can see that the results and the performance of the HEC-HMS models are robust and sufficient for the next step of the study, which is the application of the combined precipitation dataset and the calibrated model for seasonal streamflow forecasting.

The combined precipitation dataset has a similar evolution of precipitation uncertainty (standard deviation of annual areal precipitation errors) as the reference MSWEP dataset, notably in the periods before late 1990 s and early 2000 s. The median values are however higher (generally, 1 % higher), as well as the variability of standard deviation of annual areal precipitation errors among river basins. Although differences in median values are more important in the period 2005–2010, median values become comparable in the more recent period. Despite having more information available in the recent period, since satellite data is added to the TRMM-MERGE dataset, the uncertainty of the combined precipitation dataset is not reduced, as can be seen in the MSWEP dataset, which presents a decrease in the variability of the standard deviation of the errors among the river basins in the period after 1998. These differences can be explained by the fact that the MSWEP dataset uses more information and more consistent data than real time datasets. Errors and inconsistencies are often present in real time datasets, such as the ones used to build the combined dataset in this study, so it is expected that this impacts the quality of the precipitation data. Despite these issues, an important aspect of the combined precipitation dataset is that it provides a more homogeneous dataset over the region, since no regions in the study area displayed specific patterns of errors. Patterns were identified previously in the CPC and TRMM-MERGE precipitation datasets (Reis et al., 2019), with differences between the datasets growing toward the northwest of Brazil. After the combination of the datasets, the uncertainty did not show any clear dependency on the spatial location of the river basins.

The TRMM-MERGE dataset used in this study was discontinued in May 2020, and now CPTEC provides a merge product called GPM-MERGE, based on the GPM satellite product (Rozante et al., 2018; Skofronik-Jackson et al., 2018). It uses the new IMERGE retrieval algorithm, which “fuses the early precipitation estimates collected during the operation of the TRMM satellite (2000–2015) with more recent precipitation estimates collected during the operation of the GPM satellite (2014 - present)” (https://gpm.nasa.gov/data/imerg). The new CPTEC GPM-MERGE dataset maintains the same gage stations used at the TRMM-MERGE product and the same MERG algorithm (Rozante et al., 2010), which gives preference to the use of the station data over the satellite information (Rozante et al., 2020). In their study comparing the old product TMPA-V7, based on the TRMM mission, with the new products IMERGE and the GSMaP-G from JAXA, Rozante et al. (2018) found that the IMERG-E and TMPA-V7 show a similar behavior in terms of Critical success index (CSI), Adjusted Equitable Threat Score (ETS), Probability of Detection (POD), False Alarm Ratio (FAR) and Bias, with a better performance for IMERGE. These characteristics make the new GPM-MERGE the natural substitute of the discontinued TRMM-MERGE, with similar behavior, but with a better performance and higher resolution of 0.1° x 0.1°. Due the similarity of the products, we believe the results obtained in our study with the TRMM-MERGE will remain valid with the use of the new GPM-MERGE (available after May 2020).

The same is valid for the MSWEP dataset (Beck et al., 2019). The dataset used in this study is the product version V2.2, with daily precipitation data and a 0.1° spatial resolution. A comparison of the combined precipitation generated from the methodology proposed in this study with the reference MSWEP, our benchmark dataset, showed that the combined dataset has a level of uncertainty comparable with the benchmark. The examples of simulated flows showed that the calibrated models can correctly represent the long-term flow variations in different regions and climates in the study area. The MSWEP product is however in constant evolution. At the time of writing, its current version V2.8 (MSWEP V2.8 2021) provides data with daily and 3 hourly time resolutions and with the same 0.1° spatial resolution. As mentioned earlier, the complete version is still not available in real time, due to the latency of some of the products used in its production (MSWEP, 2021). However, this latency is reducing year after year, and we believe that in the next years we will have new real time products. The methodology proposed can be easily applied to consider such new products.

5. Conclusions

In this study, a sequence of steps was described that can be used to blend different real-time precipitation datasets, validate the results, and obtain a better near real-time observed precipitation forcing dataset for river basins in South America (Brazil and neighboring countries). The methodology proposed allowed us to build a long historical period of precipitation estimates at the river basin scale, which can be used in future hydrological studies such as streamflow forecasting. The main conclusion of this study is that the use of hydrological data and modeling is an asset to combine and validate precipitation datasets from different sources at large river basins in views of providing a blended dataset for hydrological applications in places where rain gauges are scarce or non-existing. Our study showed that a combination of existing precipitation datasets, weighted by the annual uncertainty of each original source, reduces precipitation uncertainty at the river basin scale. The methodology proposed allowed us to adapt, for each river basin, the proportion of each precipitation source to be considered in the combined dataset, taking thus into account the specific hydroclimatic characteristics of each river basin. The uncertainty reduction was also observed when we analyzed the results at the daily time step, with better results in terms of daily hydrological simulation when using the combined dataset than when using each precipitation source individually.

A drawback of combining data sources is the fact that datasets are often not available for the same period. In this study, we show that a possible practical solution is to extend the period of the combined precipitation dataset to cover the longest possible period, given the original datasets, by using the double-mass curve correlation. The validation of such extension was also illustrated using a hydrological model. The model allows users to evaluate, in terms of simulated discharges, if the performance of a precipitation dataset in the extended period, where not all data sources are available, remains similar and consistent to the one in the original period, where all data sources were available to build the combined precipitation dataset. Hydrological modeling proved to be a useful tool to evaluate the performance of different sources of precipitation data, as also suggested recently by Levy et al. (2017), who highlighted the importance of the problem of “data selection uncertainty” when analyzing nine datasets in Brazil.

Ongoing research focuses on the different uses of the combined precipitation dataset generated in this study. The main application is to generate ensemble members of the ESP method for seasonal streamflow forecasting and to evaluate the performance of the ESP method against streamflow forecasts based on dynamical predictions from climate models. The combined precipitation dataset will also be used to evaluate the performance of precipitation forecasts issued by meteorological (medium-range) and climate (long-range) models and, if biases are detected, to apply bias correction methods to improve these forecasts at local scales.

Author's contribution

Alberto Assis dos Reis developed the methodology, set up the datasets and models, conducted theexperiments, did the main writing of the paper. **Albrecht Weerts** contributed to the setup of the methodology through discussions with the lead author, contributed to the discussion of the results and writing the paper. **Maria-Helena Ramos** contributed to the setup of the methodology through discussions with the lead author, contributed to the discussion of the results and writing the paper. **Fredrik Wetterhall** contributed to the discussion of the results and writing the paper. **Wilson dos Santos Fernandes** contributed to the discussion of the results and writing the paper.

Declaration of Competing Interest

The authors declare that they have no known competing financial interests or personal relationships that could have appeared to influence the work reported in this paper.

Data Availability

The authors do not have permission to share data.

Acknowledgments

The first author acknowledges CEMIG - Energy Company of Minas Gerais (Companhia Energética de Minas Gerais S.A.) - Brazil for funding the research and the international visits and thanks the different institutes contributing to the research (UFMG, Brazil; INRAE, France; ECMWF, UK; Deltares, The Netherlands). We also acknowledge the data providers: NOAA - US; ONS - Brazil; CPTEC - Brazil; MSWEP - US.

Appendix A. Supporting information

Supplementary data associated with this article can be found in the online version at doi:10.1016/j.ejrh.2022.101200.

References

Adler, R.F., Huffman, G.J., Chang, A., Ferraro, R., Xie, P., Janoviak, J., Rudolf, B., Schneider, U., Curtis, S., Bolvin, D., Gruber, A., Susskind, J., Arkin, P., Nelkin, E., 2003 (doi.org/). The Version-2 Global Precipitation Climatology Project (GPCP) Monthly Precipitation Analysis (1979-Present), Vl. 4. American Meteorological Society, pp. 1147–1167. https://doi.org/10.1175/1525-7541.

Allen, R.G., Pereira, L.S., Raes, D., Smith, M., 1998. Crop Evapotranspiration - Guidelines for Computing Crop Water Requirements - FAO Irrigation and Drainage Paper 56.. ISBN 92-5-104219-5 FAO - Food and Agriculture Organization of the United Nations, Rome, p. M-56.

Arkin, P.A., Meisner, B.N., 1987. The relationship between large-scale convective rainfall and cold cloud over the western hemisphere during 1982–84. In: Mon. Weather Rev., 115, pp. 51–74.

Arnal, L., Wood, A.W., Stephens, E., Cloke, H.L., Pappenberger, F., 2017. An efficient approach for estimating streamflow forecast skill elasticity. ISSN 15257541 doi: J. Hydrometeorol. 18 (6), 17151729. https://doi.org/10.1175/JHMD160259.1. Journal of Hydrometeorology, 10, 623-643, 10.1175/2008jhm1068.1, 2009.

Beck, H.E., van Dijk, A.I.J.M., Levizzani, V., Schellekens, J., Miralles, D.G., Martens, B., de ROO, A., 2017. MSWEP: 3-hourly 0.25_ global gridded precipitation (1979–2015) by merging gauge, satellite, and reanalysis data. Hydrol. Earth Syst. Sci. 21, 589–615. https://doi.org/10.5194/hess-21-589-2017.

Beck, H.E., Wood, E.F., Pan, M., Fisher, C.K., Miralles, D.G., van Dijk, A.I.J.M., McVicar, T.R., Adler, R.F., 2019. MSWEP V2 Global 3-Hourly 0.1° Precipitation – Methodology and Quantitative Assessment. American Meteorological Society. https://doi.org/10.1175/BAMS-D-17-0138.1.

Beck, H.E., Wood, E.F., McVicar, T.R., Zambrano-Bigiarini, M., Alvarez-Garretion, C., Baez-Villanueva, O.M., Sheffield, J., Karger, D.N., 2020. Bias correction of global high-resolution precipitation climatologies using streamflow observations from 9372 catchments. J. Climatol. vol 33 (4) https://doi.org/10.1175/JCLI-D-19-0332.1.

Bennett, J.C., Wang, Q.J., Robertson, D.E., Schepen, A., Li, M., Michael, K., 2017. Assessment of an ensemble seasonal streamflow forecasting system for Australia. Hydrol. Earth Syst. Sci. 21, 6007–6030. https://doi.org/10.5194/hess-21-6007-2017.

Bennett, T.H., 1998. Development and application of a continuous soil moisture accounting algorithm for the hydrologic engineering center hydrologic modeling system (HEC-HMS). MS thesis Dept of Civil and Environmental Engineering. University of California, Davis.

Bergström, S., 1995. The HBV model. In: Singh, V.P. (Ed.), Computer Models of Watershed Hydrology. Water Resources Publications, Highlands Ranch, CO., pp. 443–476

Bitew, M.M., Gebremichael, M., Ghebremichael, L.T., Bayissa, Y.A., 2012. Evaluation of high-resolution satellite rainfall products through streamflow simulation in a hydrological modeling of a small mountainous watershed in Ethiopia. J. Hydrometeorol. 13, 338–350. https://doi.org/10.1175/2011JHM1292.1.

Cassalho, F., Rennó, C.D., Reis, J.B.C., Silva, B.C., 2020. Hydrologic validation of MERGE precipitation products over anthropogenic watersheds, 2020 Water 12 (5), 1268. https://doi.org/10.3390/w12051268.

Chen, M., Xie, P., CPC Quality Control Working Group Climate Prediction Center (CPC)/NCEP/NOAA, 2008. Quality Control of Daily Precipitation Reports at NOAA/CPC. CPC-NOAA GTS QC AMS.

Chen, Y., Weng, F., Han, Y., Liu, Q., 2008. Validation of the community radiative transfer model by using cloudsat data. J. Geophys. Res. 113, D00A03 https://doi.org/10.1029/2007JD009561.

Collischonn, B., Collischonn, W., Tucci, C.E.M., 2008. Daily hydrological modeling in the Amazon basin using TRMM rainfall estimates. J. Hydrol. 360, 207–216. https://doi.org/10.1016/j.jhydrol.2008.07.032.

Crochemore, L., Ramos, M.-H., Pappenberger, F., 2016. Bias correcting precipitation forecasts to improve the skill of seasonal streamflow forecasts. Hydrol. Earth Syst. Sci. 20, 3601–3618. https://doi.org/10.5194/hess-20-3601-2016.

Diskin, M.H., Simon, E., 1977. A procedure for the selection of objective functions for hydrologic simulation models. J. Hydrol. 34, 129–149. https://doi.org/10.1016/0022-1694(77)90066-X.

Falck, A.S., Maggioni, V., Tomasella, J., Vila, D.A., Diniz, F.L.R., 2015. Propagation of satellite precipitation uncertainties through a distributed hydrologic model: a case study in the Tocantins-Araguaia basin in Brazil. J. Hydrol. 527, 943–957. https://doi.org/10.1016/j.jhydrol.2015.05.042.

Feldman, A.D., 2000. Hydrologic Modeling System – HEC-HMS – Technical Reference Manual. USACE – US Army Corps of Engineers - Hydrologic Engineering Center, CA, USA.

Ferreira, S.A., Gan, M.A., 2011. Intraseasonal variability in the South American monsoon system. Royal Neteorological Society (wileyonlinelibrary.com) DOI:. In: Atmos. Sci. Lett., 12, pp. 253–260. https://doi.org/10.1002/asl.328.

Garreaud, R.D., Vuille, M., Rosa, C., Marengo, J., 2009. Present-day South America Climate. Palaeogeogr. Palaeoclimatol. Palaeoecol. J. 281, 180–195. https://doi.org/10.1016/j.palaeo.2007.10.032.

Gibertoni, R.F.C., Saboia, J.P.J., Daru, R.L., Kan, A., Oening, A.P., Detzel, D.H.M., Talsma, J., and Reis, A.A.: Previsão de Vazões e Operação de Reservatórios Através do Sistema Fews-CEMIG. IX CITENEL – Congresso de Inovação Tecnológica em Energia Elétrica, João Pessoa, PB - 2017.

Gilewski, P., Nawalany, M., 2018. Inter-comparison of rain-gauge, radar, and satellite (IMERG GPM) precipitation estimates performance for rainfall-runoff modeling in a mountainous catchment in Poland. Water 10, 1665. https://doi.org/10.3390/w10111665.

Golding, B.W., 2009. Long lead time flood warnings: reality or fantasy? Meteorol. Appl. 16, 3–12. https://doi.org/10.1002/met.123.

Gupta, H.V., Kling, H., Yilmaz, K.K., Martinez, G.F., 2009. Decomposition of the mean squared error and NSE performance criteria: Implications for improving hydrological modeling, 20 October J. Hydrol. Volume 377 (1–2), 80–91. https://doi.org/10.1016/j.jhydrol.2009.08.003.

Harrigan, S., Prudhomme, C., Parry, S., Smith, K., Tanguy, M., 2018. Benchmarking ensemble streamflow prediction skill in the UK. Hydrol. Earth Syst. Sci. 22, 2023–2039. https://doi.org/10.5194/hess-22-2023-2018.

Henn, B., Clark, M.P., Kavetski, D., Lundquist, J.D., 2015. Estimating mountain basin-mean precipitation from streamflow using Bayesian inference. Water Resour. Res. 51, 8012–8033. https://doi.org/10.1002/2014WR016736.

Herold, N., Alexander, L.V., Donat, M.G., Contractor, S., Becker, A., 2015. How much does it rain over land? Geophys. Res. Lett. 43, 341–348. https://doi.org/10.1002/2015GL066615.

Herrera, P.A., Marazuela, M.A., Hofmann, T., 2021. Parameter estimation and uncertainty analysis in hydrological modeling. WIREs Water Vol 9 (1). https://doi.org/10.1002/wat2.1569.

Hong, Y., Tang, G., Ma, Y., Huang, Q., Han, Z., Zeng, Z., Yang, Y., Wang, C., Guo, X., 2018. Remote sensing precipitation: sensors, retrievals, validations, and applications. Observ. Meas. Ecohydrol. Process. https://doi.org/10.1007/978-3-662-47871-4_4-1.

Huffman, G.J., Bolvin, D.T., Nelkin, E.J., 2017. Integrated Multi-satellite Retrievals for GPM (IMERG) Technical Documentation. NASA Goddard Space Flight Center, USA.

Huffman, G.J., Adler, R.F., Arkin, P., Chang, A., Ferraro, R., Gruber, A., Janowiak, J., Mcnab, A., Rudolf, B., 1997 (doi.org/). and Schneider, u. – The Global Precipitation Climatology Project (GPCP) Combined Precipitation Dataset, vl 78. American Meteorological Society, pp. 5–20. https://doi.org/10.1175/15200477.

Kirchner, J.W., 2009. Catchments as simple dynamical systems: catchment characterization, rainfall-runoff modeling, and doing hydrology backward. Water Resour. Res. 45, W02429 https://doi.org/10.1029/2008WR006912.

Klemes, V., 1986. Operational testing of hydrological simulation models. Hydrol. Sci. J. 31 (1), 13–24. https://doi.org/10.1080/02626668609491024.

Kucera, P.A., Ebert, E.E., Turk, F.J., Levizzani, V., Kirschbaum, D., Tapiador, F.J., Loew, A., Borsche, M., 2013. Precipitation from space: advancing earth system science. Bull. Am. Meteorol. Soc. 94, 365–375. https://doi.org/10.1175/BAMS-D-11-00171.1.

Kull, D., Feldman, A., 1998. Evolution of Clark's unit graph method to spatially distributed runoff. J. Hydrol. Eng. ASCE 3 (1), 9–19.

Lettenmaier, D.P., Alsdorf, D., Dozier, J., Huffman, G.J., Pan, M., Wood, E.F., 2015. Inroads of remote sensing into hydrologic science during the WRR era. Water Resour. Res. 51, 7309–7342. https://doi.org/10.1002/2015WR017616.

Levy, M.C., Cohn, A., Lopes, A.V., Thompson, S.E., 2017. Addressing rainfall data selection uncertainty using connections between rainfall and streamflow. pg. 1-12 Sci. Rep. 7, 219. https://doi.org/10.1038/s41598-017-00128-5. ⟨www.nature.com/scientificreports⟩. pg. 1-12.

Li, L., Ngongondo, C.S., Xu, C.-Y., Gong, L., 2013. Comparison of the global TRMM and WFD precipitation datasets in driving a large-scale hydrological model in southern Africa. Hydrol. Res. 44, 770–788. https://doi.org/10.2166/nh.2012.175.

Michelson, D.B., 2004. Systematic correction of precipitation gauge observations using analyzed meteorological variables (pg). J. Hydrol. 290, 161–177. https://doi.org/10.1016/j.jhydrol.2003.10.005.

MSWEP V2.8, Technical Documentation, February 14, 2021, available in ⟨https://www.dropbox.com/s/5r4nnicfe3ft12d/MSWEP_V2_doc.pdf?dl=1⟩, acessed in 2021/10/30.

Najim, M.M.M.D., 2013. Application of the HEC-HMS model for runoff simulation in a tropical catchment (pg). Environ. Model. Softw. Vl 46, 155–162. https://doi.org/10.1016/j.envsoft.2013.03.006.

Nash, J.E., Sutcliffe, J.V., 1970. River flow forecasting through conceptual models part I - a discussion of principles. J. Hydrol. 10 (3), 282–290.

ONS - Operador Nacional do Sistema Elétrico: Revisão das Séries de Vazões Naturais nas Principais Bacias do SIN – Relatório Executivo – Dezembro/2005. 126 p. Rio de Janeiro, 2005.

ONS – Operador Nacional do Sistema Elétrico: Procedimentos de Rede. 2016, available in: ⟨http://apps05.ons.org.br/procedimentorede/procedimento_rede/procedimento_rede.aspx⟩. Access at September 20th 2016.

Pozzi, W., Sheffield, J., Stefanski, R., Cripe, D., Pulwarty, R., Vogt, J.V., Heim, R.R., Brewer, M.J., Svoboda, M., Westerhoff, R., van Dijk, A.I.J.M., Lloyd-Hughes, B., Pappenberger, F., Werner, M., Dutra, E., Wetterhall, F., Wagner, W., Schubert, W., Mo, K., Nicholson, M., Bettio, L., Nunez, L., van Beek, R., Bierkens, M., Goncalves de Goncalves, L.G., Zell de Mattos, J.G., Lawford, R., 2013. Toward global drought early warning capability: expanding international cooperation for the development of a framework for monitoring and forecasting. Bull. Am. Meteorol. Soc. 94, 776–785. https://doi.org/10.1175/BAMS-D-11-00176.

Reis, A.A., Fernandes, W.S., Ramos, M.H., 2019. Assessing two precipitation data sources at basins of special interest to hydropower production in Brazil. RBRH-2019-0068 RBRH - Braz. J. Water Resour.. https://doi.org/10.1590/2318-0331.252020190068.

Rozante, J.R., Soares, M.D., Gonçalves, L.G.G., Vila, D.A., 2010. Combining TRMM and Surface Observations of Precipitation: Technique and Validation over South America, vl 25. American Meteorological Society, pp. 885–894. https://doi.org/10.1175/2010WAF2222325.1.

Rozante, J.R., Gutierrez, E.R., Fernandes, A.A., Vila, D.A., 2020. Performance of precipitation products obtained from combinations of satellite and surface observations, 2020 Int. J. Remote Sens. Vol. 41 (19), 7585–7604. https://doi.org/10.1080/01431161.2020.1763504.

Rozante, J.R., Vila, D.A., Chiqueto, J.B., Fernandes, A.A., Alvim, D.S., 2018. Evaluation of TRMM/GPM blended daily products over Brazil. Remote Sens. 10, 882. https://doi.org/10.3390/rs10060882, 2018.

Scharffenberg, W., 2016. Hydrologic Modeling System – HEC-HMS – User's Manual, version 4.2. USACE – US Army Corps of Engineers - Hydrologic Engineering Center, CA, USA.

Schwanenberg, D., Fan, F.M., Naumann, S., Kuwajima, J.I., Montero, R.A., Reis, A.A., 2015. Short-term reservoir optimization for flood mitigation under meteorological and hydrological forecast uncertainty - application to the Três Marias Reservoir in Brazil. Water Resour. Manag. 2015–29, 1635–1651. https://doi.org/10.1007/s11269-014-0899-1.

Searcy, J.K., Hardison, C.H., and Langbein, W.B.: Double-mass curves – Manual of Hydrology: Part 1. General Surface-water techniques. USGS – Geological Survey Water-Supply – Paper 1541-B, 66p, Washington, USA, 1960.

Serrat-Capdevila, A., Valdes, J.B., Stakhiv, E.Z., 2013. Water management applications for satellite precipitation products: synthesis and recommendations. J. Am. Water Resour. Assoc. 50, 509–525. https://doi.org/10.1111/jawr.12140.

Shao, Q., Traylen, A., Zhang, L., 2012. Nonparametric method for estimating the effects of climatic and catchment characteristics on mean annual evapotranspiration. Water Resour. Res. 48, W03517. https://doi.org/10.1029/2010WR009610.

Simpson, J., Adler, R.F., North, G.R., 1988. A proposed tropical rainfall measuring mission (TRMM) satellite. Bull. Am. Meteor. Soc. 69, 278. https://doi.org/10.1175/1520–0477(1988)069<0278:APTRMM>2.0.CO;2.

Siqueira, V.A., Paiva, R.C.D., Fleishmann, A.S., Fan, F.M., Ruhoff, A.L., Pontes, P.R.M., Paris, A., Calmant, S., Collischonn, W., 2018. Toward continental hydrologic-hydrodynamic modeling in South America. Hydrol. Earth Syst. Sci. Discuss. https://doi.org/10.5194/hess-22-4815-2018.

Skofronik-Jackson, G., Kirschbaum, D., Petersen, W., Huffman, G., Kidd, C., Stocker, E., Kakar, R., 2018. The global precipitation measurement (GPM) mission's scientific achievements and societal contributions: reviewing four years of advanced rain and snow observations. Q. J. R. Meteor. Soc. 144 (1), 27–48. ADVANCES IN REMOTE SENSING OF RAINFALL AND SNOWFALL, DOI: 10.1002/qj.3313, 2018.

Su, F., Hong, Y., Lettenmaier, D.P., 2008. Evaluation of TRMM multisatellite precipitation analysis (TMPA) and its utility in hydrologic prediction in the La Plata Basin. J. Hydrometeorol. 9, 622–640. https://doi.org/10.1175/2007JHM944.1.

Sun, Q., Miao, C., Duan, Q., Ashouri, H., Sorooshian, S., Hsu, H.-L., 2017. A review of global precipitation data sets: data sources, estimation, and inter-comparisons. Rev. Geophys. 56, 79–107. https://doi.org/10.1002/2017RG000574.

Tang, G., Zeng, Z., Long, D., Guo, X., Yong, B., Zhang, W., Hong, Y., 2016. Statistical and hydrological comparisons between TRMM and GPM Level-3 products over a mid-latitude basin: Is day-1 IMERG a good successor for TMPA 3B42V7? J. Hydrometeorol. 17, 121–137. https://doi.org/10.1175/JHM-D-15-0059.1.

Teweldebrhan, A.T., Burkhart, J.F., Schuler, T.V., 2018. Parameter uncertainty analysis for an operational hydrological model using residual-based and limits of acceptability approaches. Hydrol. Earth Syst. Sci. 22, 5021–5039. https://doi.org/10.5194/hess-22-5021-2018.

Tinôco, I.C.M., Bezerra, B.G., Lucio, P.S., Barbosa, L.M., 2018. Characterization of rainfall patterns in the semiarid Brazil. Anuário do Inst. De. Geociênc. – UFRJ. https://doi.org/10.11137/2018_2_397_409.

Van Osnabrugge, B., Weerts, A.H., Uijlenhoet, R., 2017. genRE - a method to extend gridded precipitation climatology data sets in near real-time for hydrological forecasting purposes. Water Resour. Res. 53 (11) https://doi.org/10.1002/2017WR021201.

Verkade, J.S., Brown, J.D., Reggiani, P., Weerts, A.H., 2013. Postprocessing ECMWF precipitation and temperature ensemble reforecasts for operational hydrologic forecasting at various spatial scales. J. Hydrol. 501, 73–91. https://doi.org/10.1016/j.jhydrol.2013.07.039.

Voisin, N., Wood, A.W., Lettenmaier, D.P., 2008. Evaluation of precipitation products for global hydrological prediction. J. Hydrometeorol. 9, 388–407. https://doi.org/10.1175/2007JHM938.1.

Wong, J.S., Yassin, F., Famiglietti, J.S., Pomeroy, J.W., 2021. A streamflow-oriented ranking-based methodological framework to combine multiple precipitation datasets across large river basins. Journal of Hydrology. Journal of Hydrology 603 (Part D), 1–19. https://doi.org/10.1016/j.jhydrol.2021.127174, 127174.

Zhang, J., Li, Y., Huang, G., Chen, X., Bao, A., 2016. Assessment of parameter uncertainty in hydrological model using a Markov-Chain-Monte-Carlo-based multilevel-factorial-analysis method. J. Hydrol. Vol 538, 471–486. https://doi.org/10.1016/j.jhydrol.2016.04.044.